

IDOCRASE: SYNTHESIS, PHASE RELATIONS  
AND CRYSTAL CHEMISTRY<sup>1</sup>JUN ITO AND JOEL E. AREM, *Department of Geological Sciences,  
Harvard University, Cambridge, Massachusetts 02138.*

## ABSTRACT

Phase syntheses of Mg-idocrase indicate that the mineral's compositional range may be written as  $\text{Ca}_{18}(\text{Ca}_{2-x}\text{Mg}_x)\text{Mg}_2(\text{Mg}_{2-y}\text{Al}_y)\text{Al}_8(\text{Al}_y\text{Si}_{2-y})\text{Si}_{16}\text{O}_{68}(\text{OH})_8$  where  $0.0 \leq x < 1.5$  and  $0.0 < y < 1.5$ .  $\text{Mg}^{2+}$  ions in 6-coordinated sites seem to be essential for idocrase formation, unlike the case for grossular garnet.

Pressure-temperature stability fields under pure water in the sodium-free system are wide. With water pressures of 2 kbar, idocrase is stable from 450°C to 720°C.

The mineral associations of idocrase (in contact metamorphism) can be ideally illustrated as follows: 2 grossular + 2 diopside + wollastonite + calcite + 2 water = idocrase + 2 quartz +  $\text{CO}_2$ . The presence of three mineral zones (garnet, idocrase and monticellite) at Crestmore, California, is best explained in terms of compositional changes, rather than pressure-temperature variation.

Unit cell dimensions of  $\text{Mg}^{2+}$ ,  $\text{Ni}^{2+}$ ,  $\text{Co}^{2+}$  and  $\text{Cu}^{2+}$  analogs and those of Mg-Idocrase which also contained  $\text{Fe}^{3+}$ ,  $\text{Mn}^{2+}$  or  $\text{Ti}^{4+}$  were obtained from computer-refined X-ray powder diffractometer data. Mg-idocrase with the formula  $\text{Ca}_{18.6}\text{Mg}_{3.2}\text{Al}_{10.1}\text{Si}_{17.6}\text{O}_{68}(\text{OH})_8$  (electron probe analysis) has unit cell dimensions:  $a = 15.600 \pm 0.001 \text{ \AA}$ ;  $c = 11.829 \pm 0.002 \text{ \AA}$ .

Qualitative kinetics studies showed that the rate of growth and nucleation of idocrase are strongly dependent on temperature and pressure. The use of different gel compositions, and of various starting materials, demonstrates the diversity of kinetic processes in idocrase crystallization.

## INTRODUCTION

Idocrase occurs principally in contact metamorphic zones associated with limestones, where it is commonly found with garnet (grossular), diopside, wollastonite, and calcite. Idocrase is also found in regionally metamorphosed limestones, in veins and pockets associated with basic and ultrabasic rocks, and in nepheline syenites. The occurrence at Mt. Vesuvius (from which Werner derived the name vesuvianite) is in ejected dolomite blocks. The diversity of conditions demonstrated by these occurrences indicates that idocrase is stable over a considerable range of crustal temperatures and pressures.

Previous experimental investigations were carried out by Coes (1955), Rapp and Smith (1958), Christophe-Michel-Lévy (1960), Christie (1961), and Walter (1966). Data on idocrase synthesis are summarized in Table 1 and suggest a broad field of stability for the mineral.

Idocrase is chemically very similar to grossular garnet, but the differences in composition can be clearly demonstrated by plotting analyses on a  $\text{SiO}_2\text{—Al}_2\text{O}_3\text{—}(\text{Ca, Mg})\text{O}$  diagram (McConnell, 1939) or on an

<sup>1</sup> Mineralogical Contribution No. 476.

TABLE 1. CONDITIONS FOR THE PREVIOUSLY-REPORTED IDOCRASE SYNTHESSES

Author, and suggested formula	Method	T°C	P kbar	Duration	Starting materials
Coes (1955) $\text{Ca}_{10}(\text{Mg, Fe})_2\text{Al}_4\text{Si}_9\text{O}_{34}(\text{OH})_4$	High pressure apparatus	700°	10.0	—	Kaolin, $\text{Ca}(\text{OH})_2$ , $\text{MgCl}_2 \cdot 6\text{H}_2\text{O}$
Rapp and Smith (1958) $\text{Ca}_{10}\text{Al}_8\text{Si}_7\text{O}_{34}(\text{OH})_4$	Hydrothermal	550–600°	1.5–2.5	—	Gel-mix
Cristophe Michel-Lévy (1960) $\text{Ca}_{10}\text{Mg}_2\text{Al}_4\text{Si}_9\text{O}_{34}(\text{OH})_4$	Hydrothermal	450–500°	0.5–1.0	—	$\text{CaCO}_3$ , $4\text{MgCO}_3$ , $\text{Mg}(\text{OH})_2 \cdot 6\text{H}_2\text{O}$ Amorphous silica and alumina.
Walter (1966) $\text{Ca}_{19}\text{Al}_{10}(\text{Al, Mg})_4\text{Si}_{17}\text{O}_{68}(\text{OH})_4(\text{O, OH})_4$	Hydrothermal	558°C	4–5.5	10 weeks	Gel-mix
Christie (1961) $\text{Ca}_{10}\text{Mg}_2\text{Al}_4\text{Si}_9\text{O}_{34}(\text{OH})_4$	Hydrothermal	509°	6.7	10 weeks	Åkermanite and gehlenite

ACF ( $\text{Al}_2\text{O}_3$ —CaO—(Mg, Fe)O) projection (Barth, 1963). Most existing analyses, except for a few, some of which may be unreliable, define a clearly-outlined field of composition on the ACF diagram. The “ideal” chemical formula, however, as proposed from a structure analysis by Warren and Modell (1931), departs slightly from the majority of natural idocrase analyses. The Warren-Modell formula, which can be written as  $\text{Ca}_{20}\text{Mg}_4\text{Al}_8\text{Si}_{18}\text{O}_{68}(\text{OH})_8$ <sup>1</sup> was challenged by Machatschki (1932) because of the apparent departure from observed compositions. Machatschki proposed an alternative formula  $\text{Ca}_{19}(\text{Mg, Fe}^{2+}, \text{Fe}^{3+}, \text{Al})_{13}\text{Si}_{18}(\text{O, OH, F})_{76}$ , but this is essentially the same as that of Warren and Modell. Barth (1963) suggested a general formula  $X_{10-u}Y_{6+u}Z_9(\text{O, OH, F})_{38}$ , where  $X = \text{Ca, Mn, Na, K}$ ;  $Y = \text{Mg, Fe, Ti, Al, Cu}$ ; and  $Z$  is mostly Si, with small amounts of Al. With  $u \leq 1$ , the formula agrees well with the results of chemical analyses of Norwegian idocrase. The recent phase equilibrium study by Walter (1966) involving the system  $\text{CaO}$ — $\text{MgO}$ — $\text{Al}_2\text{O}_3$ — $\text{SiO}_2$ — $\text{H}_2\text{O}$  produced another “working” formula,  $\text{Ca}_{19}\text{Al}_{10}(\text{Al, Mg})_4\text{Si}_{17}\text{O}_{68}(\text{OH})_4(\text{O, OH})_4$ , again essentially the same as the original “structural” formula of Warren and Modell (1931).

<sup>1</sup> In the present study we have found the most convenient chemical-structural unit to be 1/2 unit cell (where  $Z = 4$ ) and all formulas have been so written.

None of the above formulas agrees with all published analyses of idocrase. This mineral remains one of a small number of rock-forming silicates whose formula and structure are not fully established. Thus, there exists a problem which can only be solved by means of modern crystal structure refinement, using carefully analyzed homogeneous natural material (J. Arem, in progress) or a synthetic crystal of known chemical composition.

The present work was originally undertaken in an attempt to grow single crystals of idocrase of known composition for crystal structure analysis, and the results of preliminary synthesis studies for two compositions are reported in this paper. Such studies are necessary prior to successful crystal growth. The relatively low temperature-pressure ranges used (350 to 750°C, 250 to 3,000 bar) were imposed by limited facilities. This range also seems to be realistic in terms of natural occurrences of idocrase. Moreover, equipment for growth of large single crystals operates well under such conditions.

It is anticipated that the substitution of atomic species in various sites in the idocrase structure will be of some interest to crystal chemists. Furthermore, this structure is remarkably similar to that of garnet (Warren and Modell, 1931; J. Arem, in progress), and the usefulness of such substitutions in solid state applications of garnets is well known. Several new idocrase analogs with transition elements have been synthesized.

The kinetics of hydrothermal crystallization were studied in some detail, partly because knowledge of such processes may lead to better understanding of the formation of idocrase in nature.

#### EXPERIMENTAL PROCEDURE

*Starting Materials.* (1) Reactive sodium-free<sup>1</sup> gels used in this study were prepared with the following: reagent grade analyzed  $Mg(OH)_2$  powder;  $Al(OH)_3$ , freshly prepared by treating reagent grade aluminum nitrate solution with ammonia; reagent grade  $Ca(OH)_2$  powder; and a pure silicic acid solution prepared using a cation exchange resin (Ito and Johnson, 1968). The above hydroxides were added to warm silicic acid solution (approx. 0.1 M) in the above order at intervals of 15 minutes, and stirred with a magnetic stirrer. The solution containing dispersed hydroxides gelatinized when it became alkaline with the addition of  $Ca(OH)_2$  (approx. pH 9). The homogenized gels were dried in an oven at 140°C. Chemical analyses of the gel showed that it contains 20–25 percent  $H_2O$  and 0.04 percent  $Na_2O$  in addition to the necessary four oxide components. X-ray powder diffraction of this gel gave a weak but distinct pattern of hydrogarnet ( $a = 12.43 \text{ \AA}$ ) and a minor peak due to calcite. A small amount of  $CaCO_3$  did not interfere with the present experiments; however,  $CaCO_3$ -free gel can be prepared under a  $CO_2$ -free atmosphere. A Teflon container with 500 ml capacity is sufficient to prepare approximately 2 g of the dried gel.

<sup>1</sup> Sodium-free hereafter indicates  $Na_2O < 0.05$  percent.

(2) Sodium-containing coprecipitated gels were prepared from solutions containing calcium nitrate, aluminum nitrate, magnesium nitrate and sodium silicate, at a pH of over 14. In this pH range, Ca ions remain in the precipitates. The precipitates were centrifuged, and washed twice with distilled water to reduce adsorbed sodium to the desired level. A considerable amount of aluminum was recovered from the washing solution by lowering its pH to 7 using hydrochloric acid and ammonia. The recovered  $\text{Al}(\text{OH})_3$  was washed twice with distilled water and centrifuged.

These two precipitates were combined and stirred in a porcelain evaporating dish using a magnetic stirrer, and then dried in an oven at  $140^\circ\text{C}$ . This precipitated gel is amorphous. A chemical analysis of the gel showed approximately 20 percent  $\text{H}_2\text{O}$  and 5–6 percent  $\text{Na}_2\text{O}$  in addition to the necessary amounts of four essential components. The accuracy of the mixing ratio of the gel method usually is not as good as with the direct mixing of analyzed oxides or hydroxides. If there is not a considerable difference in the reaction time, the latter method may be preferable.

(3) The starting gels for several new idocrase analogs, such as those containing Cu, Co and Ni were prepared using the above two methods.  $\text{NiCO}_3$ ,  $\text{CoCO}_3$  and  $\text{CuCO}_3 \cdot \text{Cu}(\text{OH})_2$  were used, replacing  $\text{Mg}(\text{OH})_2$  powder in method (1), and Cu, Ni and Co nitrates were dissolved into the solutions instead of magnesium nitrate when the precipitation method (2) was chosen.  $\text{MnCO}_3$ ,  $\text{Zn}(\text{OH})_2$ ,  $\text{Be}(\text{OH})_2$ , freshly prepared titanium hydrated oxide, and ferric hydroxide were also used for certain experiments.

(4) Starting mixtures of dry oxides and hydroxides were made simply by mixing desired amounts of the standardized reagents using a mechanical mortar for 2 hours. In some cases, hygroscopic oxides were heated at  $1,000^\circ\text{C}$  for 20 hours before mixing.  $\text{CaCO}_3$  was used in some experiments, but it delayed considerably the time needed for completion of the reactions.

*Synthesis.* Approximately 60 mg of the starting materials were placed in a silver foil capsule ( $3\text{ cm} \times 3\text{ cm} \times 0.03\text{ cm}$ ) for the short-term runs ( $<5$  days). For runs of more than 5 days duration, welded silver tubing (5 mm diameter) and gold tubing (2.5 mm diameter) was used. The capsules were heated in a cold seal bomb of 10 ml capacity. Sufficient water was added to maintain the  $\text{H}_2\text{O}$  pressures (250 to 3,000 bar) during the runs. Vertical tube furnaces (10 cm diameter and 45 cm long) with kanthal<sup>1</sup> wire were used for heating at temperatures ranging from 300 to  $750^\circ\text{C}$ . Temperatures were regulated to within  $\pm 5^\circ\text{C}$  with an on-off controller-programmer and Pt–Pt+10% Rh thermocouple. Temperature readings were periodically checked using a digital millivoltmeter. At the end of the runs, the bomb was quenched, and the samples were washed out of the capsules and air dried. The pH of the residual liquids in the silver capsules was checked using pH paper. Resulting pH values were as follows: Na-containing gel:  $\approx 9.5$ ,  $\text{Ca}(\text{OH})_2$  gel:  $\approx 8.5$ ,  $\text{CaCO}_3$  gel and the other oxide and hydroxide mixtures:  $\approx 7.0$ .

Following several runs which were made at  $650^\circ\text{C}$  and 1.5 kbar for 48 hours, the fluid remaining in the bomb was analyzed using an atomic absorption flame photometer (Perkin Elmer 303). The concentrations found for the four essential components Ca, Al, Mg and Si were no more than those found in blank runs. Therefore, it appears that no significant amount of starting material was lost to the fluid from the capsules during the runs. Natural idocrase crystal fragments (0.25 g carefully weighed and wrapped in silver foil) lost no weight after 48 hours at  $650^\circ\text{C}$ , 1.5 kbar  $\text{H}_2\text{O}$  pressure. Possible contamination by iron or

<sup>1</sup> Kanthal A-1: Iron-chromium-aluminum-cobalt electrical resistance heating alloy.

other metals was checked using emission spectrographic analysis. The iron content of the run products did not exceed the level usually detected in the reagent grade chemicals used in this study. No other elements were found in significant amounts.

Several runs were made in the range of 250–550°C and 5 and 8 kbar using gels and an opposed-anvil pressure device. The very minute quantities of products obtained during the dry press runs and their somewhat poor crystallinity prevented us from examining these samples in detail.

All the run products were examined by X-ray powder diffraction using Ni-filtered Cu radiation. The results of syntheses are deposited with the National Auxiliary Publication Service, American Society for Information Service.<sup>1</sup>

#### PRESSURE-TEMPERATURE-COMPOSITION-STUDIES

*Fixed composition.* The formula and structure of idocrase and the extent of substitution in the various structural sites has not yet been fully established. Any phase equilibrium study at a fixed chemical composition will represent only one cross section of the pressure-temperature-composition diagram of the multi-component system representing possible idocrase compositions.

Phase synthesis experiments were carried out at temperatures of 300 to 750°C and water pressures of 250 to 3,000 bar. The first experiments used a sodium-free gel having the composition  $\text{Ca}_{20}\text{Mg}_4\text{Al}_8\text{Si}_{18}\text{O}_{68}(\text{OH})_8 \cdot n\text{H}_2\text{O}$ . This composition was chosen from various possible formulas because (1) it represents the ideal formula given by Warren and Modell (1931), (2) a rapid preliminary survey had shown that it has a relatively wide pressure-temperature stability range compared with other compositions studied here, and (3) it crystallizes more rapidly than other compositions to a nearly single-phase idocrase (see following section). The results for this composition are given in Figure 1a.

Two additional synthesis studies, one in Na-containing (Fig. 1b) and one in Na-free environments, gave results nearly identical to the first. The gel for the second and third studies had a chemical composition  $\text{Ca}_{19}\text{Mg}_4\text{Al}_{10}\text{Si}_{17}\text{O}_{68}(\text{OH})_8 \cdot n\text{H}_2\text{O}$ , and the oxide ratio of its four cation components was similar to that of most naturally-occurring idocrase.

The boundaries in Figures 1a and 1b between idocrase and the high-temperature assemblage (which consists mainly of mellite, but contains small amounts of wollastonite and monticellite), both have positive slopes. These do not appear to differ significantly for the two compositions. At high  $P$ - $T$  ranges, a monticellite-predominant region probably exists. Decomposition (or dehydration) temperatures in the highly

<sup>1</sup> Order NAPS Document #00945 from National Auxiliary Publications Service of A.S.I.S., c/o CCM Information Corporation, 909 Third Avenue, New York, N. Y. 10022, remitting \$2.00 for microfiche or \$5.00 for photocopies, in advance payable to CCMIC-NAPS.

alkaline environment (Fig. 1b) are approximately 40°C lower than those in the sodium-free environment (Fig. 1a). The high-temperature stability limits of idocrase are shown dotted in both figures because H<sub>2</sub>O pressures for the runs were not measured accurately, and slight errors in these positive slopes could thus be expected. However, the basic shapes of these boundaries would not be altered.

The reversibility of the melilite-idocrase boundary at high temperatures has been established. Melilite synthesized at 720°C, 500 bar decomposed to idocrase at 650°C, 1.8 kbar and also at 600°C, 1.0 kbar. The sluggishness of the reaction prevented complete reformation of idocrase from the breakdown products in the low-temperature runs.

CO<sub>2</sub> activity was not considered throughout the experimental work, since only in its final stages did we realize that this variable has a significant effect upon idocrase stability. The idocrase-predominant region can still be established reasonably well, even though slight variations in stoichiometry of the starting materials (owing to losses in gel preparation) result in the appearance of additional phases within this *P-T* region.

The low-temperature equilibrium boundaries are also drawn as dotted lines, and are somewhat tentative. Low crystalline yields and poor crystallinity suggest that the lower pressure and temperature runs have not completely equilibrated within the duration set for the present experiments (maximum, 5 days). The low temperature boundaries might shift further toward lower temperatures by as much as 50°C or more in runs of longer duration. The lower equilibrium temperature under high pressures (6.7 kbar) reported by Christie (1961) for idocrase-hydrogarnet is consistent with our present experiments. However, reaction reversal experiments in our work did not confirm the presence of hydrogarnet at only 1 kbar and 300°C.

At temperatures below the idocrase field the phase assemblage consists mainly of hydrogarnet ( $a=11.97 \text{ \AA}$ ), with diopside (in the high pressure range) and with various hydrated calcium silicates such as xonotlite or plombierite in the low pressure range. Idocrase is stable at lower temperatures (by approx. 60°C) in a strongly alkaline environment (Fig. 1b). This difference in the stability fields is largely caused by the alkaline environment during the hydrothermal heating. The effects of changing the ratio of the other four components seem less prominent than those due to the presence of sodium.

It seems worth noting that grossular often appeared at the high-temperature equilibrium boundaries, especially in the Al-rich runs. This probably is due to the fact that the dehydration of idocrase occurs within the stability range of grossular. The runs shown as X in the lower pres-

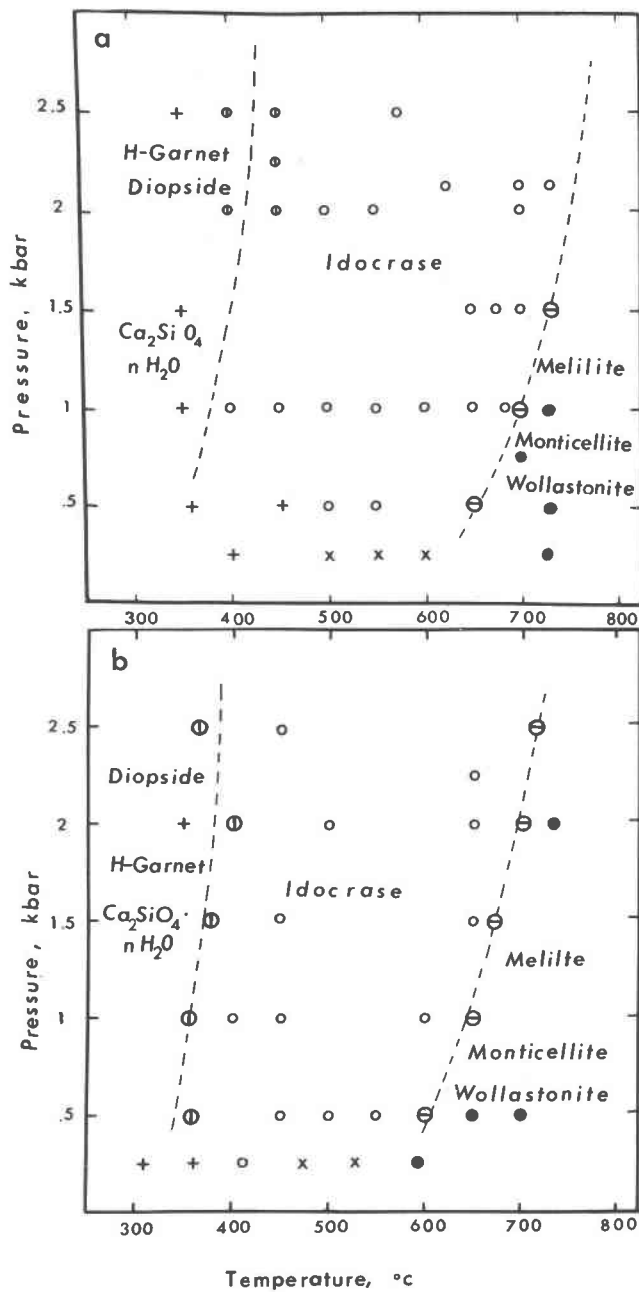


FIG. 1a. Pressure-temperature diagram for synthesis runs for gel composition  $\text{Ca}_{20}\text{Mg}_4\text{Al}_8\text{Si}_{18}(\text{OH})_8 \cdot n\text{H}_2\text{O}$ , in an alkali-free environment at 300–800°C and 0–3 kbar.

sure range of Figures 1a and 1b contain hydrogrossular ( $a = 11.92 \text{ \AA}$ ), idocrase, wollastonite and melilite. These runs might not have equilibrated, and some of the phases are probably metastable.

Our results show that the pressure-temperature stability region for idocrase with optimum chemical compositions (under water pressure) is remarkably wide, and that the idocrase structure can be stabilized at temperatures as low as  $360^\circ\text{C}$  at 500 bar, and will remain stable up to  $800^\circ\text{C}$  at 10 kbar (Coes, 1955). All the data from previously described work on the syntheses of idocrase fall within this region. Furthermore, this  $P$ - $T$  range is compatible with pressures and temperatures estimated for natural occurrences.

However, one has to bear in mind that the experiments carried out under conditions where  $P_{\text{H}_2\text{O}} \approx P_{\text{Tot}}$ , do not sufficiently simulate the formation of all idocrase in nature, because its prime occurrence is in contact metamorphic zones, where the  $\text{CO}_2$  activity cannot be ignored. With appreciable  $\text{CO}_2$  activity, the upper-left (high pressure and low temperature) part of the idocrase  $P$ - $T$  diagram (under  $\text{H}_2\text{O}$  pressure, Figs. 1a and 1b) will be dominated by a mixed-phase region consisting mainly of grossular, diopside and calcite. As evidence for this conclusion we have found that experiments using starting materials containing calcite as the Ca source material, with excess organic acid such as ascorbic acid (which decomposes to  $\text{CO}_2$  and  $\text{H}_2\text{O}$ ) do not, in general, yield idocrase throughout the  $P$ - $T$  range studied. However, in a narrow overlap region in which pure calcite and quartz react to form wollastonite (Greenwood, 1962) under  $\text{CO}_2$ -pressure, we still expect to find idocrase, even if the activity of  $\text{CO}_2$  is considerable. Further investigations in a buffered system would lead to a better understanding of the contact metamorphic occurrences of idocrase.

*Compositional studies at fixed  $P$  and  $T$ .* Most previous reports of idocrase

---

○ = idocrase; ● = high temperature assemblage, mainly melilite with small amounts of wollastonite and monticellite; ⊕ = two-phase region, of idocrase+hydrogarnet; + = low temperature assemblage, hydrogarnet-diopside- $\text{Ca}_2\text{SiO}_4 \cdot n\text{H}_2\text{O}$ ; × = low pressure assemblage idocrase-grossular-melilite-wollastonite; ⊖ = two-phase assemblage melilite+idocrase.

FIG. 1b. Pressure-temperature diagram for synthesis runs for the gel of composition  $\text{Ca}_{13}\text{Mg}_4\text{Al}_{10}\text{Si}_{17}\text{O}_{68} \cdot n\text{H}_2\text{O}$  in a strongly alkaline environment at  $300$ – $800^\circ\text{C}$  and  $0$ – $3$  kbar. ○ = idocrase; ● = high temperature assemblage, mainly melilite with a small amount of monticellite and wollastonite; ⊖ = two-phase assemblage idocrase+melilite; ⊕ = two-phase assemblage, idocrase-hydrogarnet; + = low temperature assemblage of hydrogrossular-diopside- $\text{Ca}_2\text{SiO}_4 \cdot n\text{H}_2\text{O}$ ; × = low pressure assemblage idocrase-grossular-melilite-wollastonite.

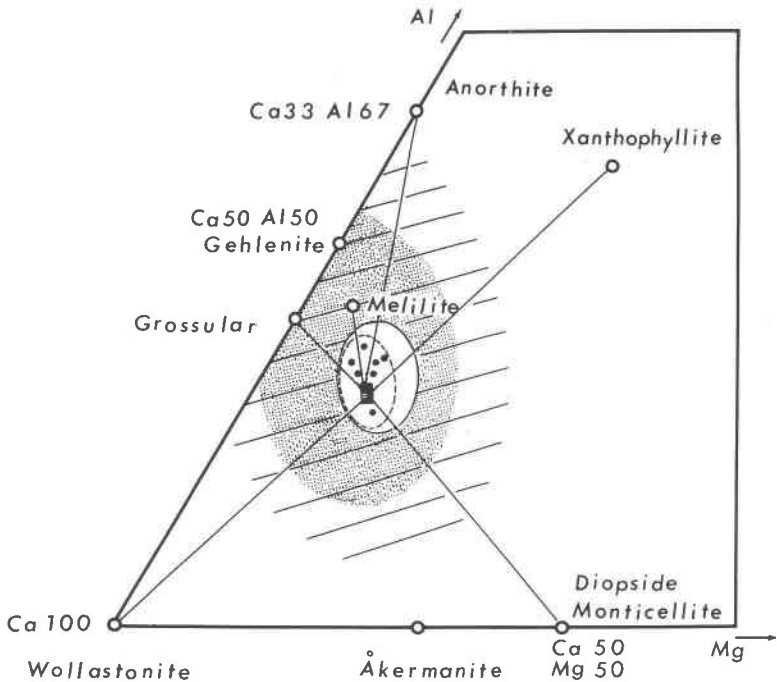


FIG. 2. Two superimposed isothermal-isobaric sections of partial ACF diagrams showing the stable compositional range for idocrase. Dark square = synthetic idocrase; black dots represent analyses of natural idocrase. Area encircled by dotted line is idocrase-predominant region, and stippled area is partially superimposed phase region (both in the Na-free system at 650°C, 1.5 kbar). Area encircled by solid line is idocrase-predominant region, and shaded area is partially superimposed phase region (both in the Na-containing system at 550°C, 2 kbar).

synthesis (Rapp and Smith, 1958; Cristophe-Michel-Lévy, 1960; Christie 1961; Walter, 1966) mention the appearance of other phases, such as grossular, diopside, anorthite and zoisite. A preliminary investigation was therefore conducted in the system  $\text{H}_2\text{O}-\text{MgO}-\text{CaO}-\text{Al}_2\text{O}_3-\text{SiO}_2$ , in order to locate the compositional region in which idocrase appears as a single phase, and to reveal the extent of any solid solution (suggested by the previous studies) for the mineral within this system. Two different sets of experiments were performed, one at 650°C and 1.5 kbar using sodium-free gel, and the other at 550°C and 3 kbar using sodium-containing gel.

The results permit us to construct a partial ACF ( $F = \text{Mg}$ ) diagram (Fig. 2). In this diagram, we are able to locate a small region (the space encircled with a dotted line is for 650°C, 1.5 kbar, and with a solid line

for 550°C, 2 kbar) in which idocrase is the predominant synthesis product. A smaller black square within these regions was plotted using the results of electron microprobe analyses of idocrase single crystals obtained from the gel of composition  $\text{Ca}_{19}\text{Mg}_4\text{Al}_{10}\text{Si}_{17}\text{O}_{68}(\text{OH})_8$ . A small difference between actual crystal composition and the starting composition has been noted (see following section).

Shaded areas (lines and stipples) in these diagrams indicate the compositional ranges for the present study. These consist of partially superimposed regions of the adjacent phases, as viewed in projection.

Most of the existing chemical analyses of idocrase plot within the idocrase-predominant regions (inside dotted line) and trend more toward the relatively aluminum-rich side of the diagram. These analyses are designated by black circles in Figure 2. All divalent ions (excluding Ca) and trivalent ions were plotted as Mg and Al, respectively. In the sodium-containing system the idocrase-predominant region expands in size and shifts appreciably toward the Al-rich side compared to its position in the sodium-free system. This probably arises because excess Al in the gel is dissolved in strong NaOH hydrothermal fluids. The remaining gel, without excess Al, crystallizes an idocrase denuded in Al compared with the original bulk gel composition. Thus, idocrase may appear in Na-bearing runs at compositions where grossular or melilite become major constituents of the Na-free system.

The phases identified in the compositional range studied here are wollastonite, diopside, monticellite, grossular, melilite and xanthophyllite for the experiments at 650°C and 1.5 kbar, using Na-free gels. Those in the sodium-containing system at 550°C and 2 kbar are grossular, diopside, monticellite and xanthophyllite (most of the sodium in the system remained in the hydrothermal fluid). Calcite often exists stably in all of these assemblages.

A few additional experiments were carried out by simply adding or subtracting some Si from the gel composition  $\text{Ca}_{19}\text{Mg}_4\text{Al}_{10}\text{Si}_{17}\text{O}_{68}(\text{OH})_8$ . Run products showed the immediate appearance of additional phases, such as grossular or diopside, with one Si atom added to the above formula. Monticellite, melilite and xanthophyllite appeared when a formula having two fewer Si atoms was used.

From the results above, we believe that a narrow but distinct region of solid solution for idocrase does exist. The compositional distinction between idocrase and grossular, and the relationship between idocrase and other phases, are depicted in a quaternary diagram of the  $\text{MgO}-\text{CaO}-\text{Al}_2\text{O}_3-\text{SiO}_2$  system (Fig. 3). The diagram was drawn from a model, built using the technique of Arem (1967). A standard ACF projection of this diagram, using oxide components, was described by Turner and Ver-

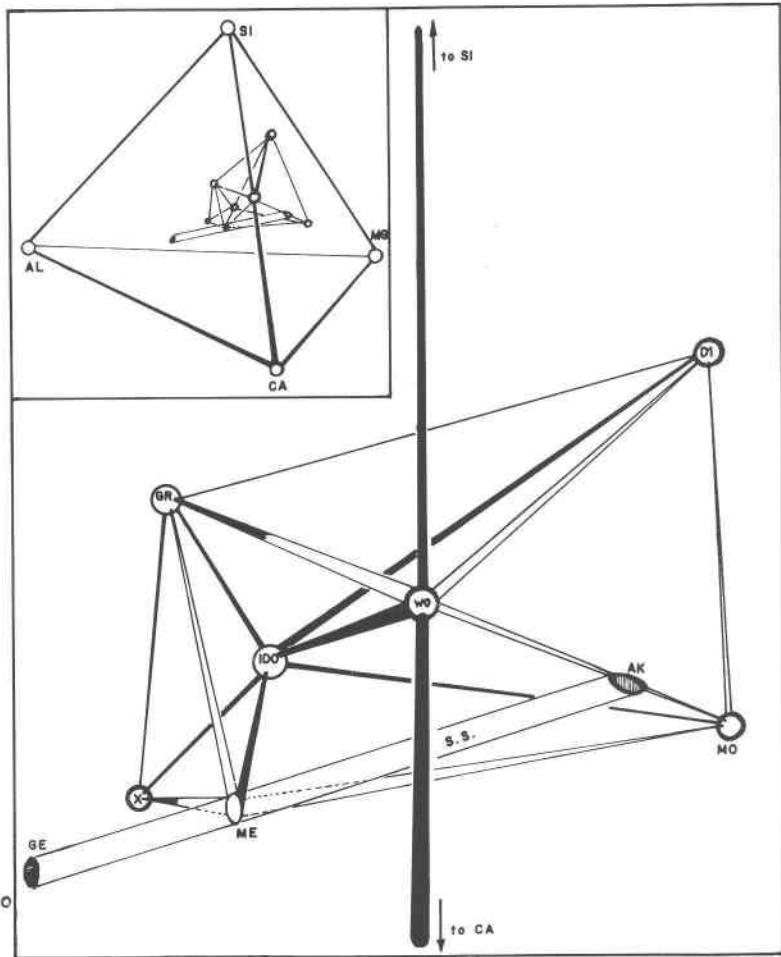


FIG. 3. Portion of the system Al—Ca—Mg—Si (projected through oxygen) including the phases appearing in alkali-free experiments. Lines joining phases are not necessarily stability tie-lines. Areas at phase locations do not necessarily represent the extent of solid solution. Ak=åkermanite; Di=diopside; Ge=gehlenite; Gr=grossular; Ido=idocrase; Me=melilite; Mo=monticellite; S.S.=solidid solution; Wo=wollastonite; X=xanthophyllite.

hoogen (1960). The projected idocrase solid solution field may be curved and possibly represented in the quaternary diagram by a flattened ellipsoid. Its composition range fits well the following tentative formula:



where  $0.0 \leq y < 1.5$ ;  $0.0 \leq x < 1.5$ .

The above formula (based on 152 oxygens per unit cell) covers reasonably well most of the new and old chemical analyses of natural specimens. Differences observed among unit-cell dimensions within the range are somewhat small (see Table 4). It is possible, that hydroxyl or halogen site vacancies (Walter, private communication) balance Mg-Al substitution (Shabynin, 1968). However, under hydrothermal conditions, where hydroxyl ions are abundant, hydroxy-oxy substitution (missing hydrogen in OH sites) seems less likely, and cationic replacements seem more likely.

Mg-free idocrases reported by both Rapp and Smith (1958) and Christophe-Michel-Lévy (1960) were not confirmed by Walter (1966) or by the present study. Our stable region for idocrase in the compositional (*ACF*) diagram fell short of reaching both the formula of Rapp and Smith:  $\text{Ca}_{20}\text{Al}_{16}\text{Si}_{14}\text{O}_{68}(\text{OH})_8$ , and that of Christophe-Michel-Lévy;  $\text{Ca}_{20}\text{Al}_{12}\text{Si}_{18}\text{O}_{68}(\text{OH})_8$ . From both compositions, only grossular was obtained as a dominant phase under the diverse conditions of our experiments.

Part of a later section outlines the results of kinetic studies on nine selected gel compositions in the region in which idocrase is predominant. These studies substantiate our proposed solid-solution range for idocrase. We note here merely that the appearance of metastable phases and rates of crystallization vary with composition and conditions of synthesis.

No working formula, supported only by analyses and other experimental observations, can provide complete crystal chemical knowledge about a mineral species. In view of the structural refinement now in progress (Arem), further speculation does not seem justified at this time.

#### MICROPROBE ANALYSES

Analyses were performed on several samples of each synthetic idocrase and on natural idocrase crystals. Inasmuch as the chemical composition of starting materials may not be the same as that of a run product, it was necessary to obtain analytical data on the synthetic idocrase. Moreover, the possibility of contamination by extraneous sodium or iron had to be examined. All specimens were mounted as polished sections in epoxy, and all samples and standards were carbon-coated simultaneously. Instrumental conditions were as follows: Applied Research Laboratories EMX Microprobe, accelerating voltage 20 kV, beam current 0.023  $\mu\text{A}$  (on sample). A correction for drift was made automatically by using fixed count of backscatter electrons rather than fixed time, but drift was found to be negligible throughout the course of analysis. At least 10 counts were made on each sample; normally several repeat counts were made on each of several crystals, and these results were averaged.

TABLE 2. RESULTS OF ELECTRON PROBE ANALYSIS OF SYNTHETIC MG-IDOCRASE,  
USING STARTING MATERIALS HAVING THE COMPOSITION  
 $\text{Ca}_{19}\text{Mg}_4\text{Al}_{10}\text{Si}_{17}\text{O}_{68}(\text{OH})_8$

Starting mixtures	SiO <sub>2</sub>	Al <sub>2</sub> O <sub>3</sub>	MgO	CaO	Fe <sub>2</sub> O <sub>3</sub>	Na <sub>2</sub> O
1. CaCO <sub>3</sub> , oxides+NaHCO <sub>3</sub>	37.3	18.4	4.5	36.0	0.0x	0.13
2. Ca(OH) <sub>2</sub> , Mg(OH) <sub>2</sub> +Al-silicate (Gel)	37.0	18.0	4.5	36.4	0.0x	0.1
3. CaCO <sub>3</sub> , Mg(OH) <sub>2</sub> +Al-silicate (Gel)	36.5	19.2	4.0	36.0	0.0x	0.1
4. Synthetic idocrase analyzed by Walter (1966) (mean of 5 analyses)	36.9	19.8	4.2	37.0	—	—
5. Idocrase from Asbestos, Que. (pale green)	37.1	19.1	2.8	36.7	1.53	0.1
6. Idocrase from Sanford, Maine	36.6	17.7	2.2	35.9	4.65	0.25

Calculated formulas:

1.  $\text{Ca}_{18.2}\text{Mg}_{3.2}\text{Al}_{10.2}\text{Si}_{17.6}\text{O}_{68}(\text{OH})_8$
2.  $\text{Ca}_{18.6}\text{Mg}_{3.2}\text{Al}_{10.1}\text{Si}_{17.6}\text{O}_{68}(\text{OH})_8$
3.  $\text{Ca}_{18.3}\text{Mg}_{2.8}\text{Al}_{10.8}\text{Si}_{17.4}\text{O}_{68}(\text{OH})_8$
4.  $\text{Ca}_{18.5}\text{Mg}_{2.9}\text{Al}_{10.9}\text{Si}_{17.2}\text{O}_{68}(\text{OH})_8$
5.  $\text{Ca}_{18.6}\text{Na}_{0.1}\text{Mg}_{2.6}\text{Fe}_{0.5}\text{Al}_{10.6}\text{Si}_{17.6}\text{O}_{68}(\text{OH})_8$
6.  $\text{Ca}_{18.2}\text{Na}_{0.2}\text{Mg}_{1.6}\text{Fe}_{1.7}\text{Al}_9\text{Si}_{17.6}\text{O}_{68}(\text{OH})_8$

Grossular garnets were used as standards for Al, Mg, Ca and Si analyses, since garnet and idocrase are chemically very similar. Plagioclase feldspars were used to establish a working curve for Na, and matrix effects in most cases are believed to be insignificant. Good standard curves were obtained for most elements determined.

Satisfactory results were obtained on several idocrase crystals grown to fairly large size from starting materials having the composition  $\text{Ca}_{19}\text{Mg}_4\text{Al}_{10}\text{Si}_{17}\text{O}_{68}(\text{OH})_8$ , which is seen to lie near the center of the idocrase stability field. Some of the analytical results are given in Table 2.

One of the original aims of the present study was to find conditions suitable for the growth of large idocrase crystals. A first step towards this goal must be to determine the *P-T-X* region of stability of the material being investigated. However, experiments conducted within this region, although efficient in producing the desired phase, are distinguished by abundant nucleation. This process limits crystal size; in fact, the normal crystal size encountered in these circumstances is on the order of 1–5  $\mu\text{m}$ . Since our initial experiments were aimed at defining an idocrase-predominant stability field, most of the yields of our runs contained abundant minute crystals. Although a 1  $\mu\text{m}$  beam was used in the probe work, many of the samples exhibited such small crystal size that the sums of analytical results were consistently low, and these were not reported here. This was true especially of the idocrase synthesized from Na-bearing gels (which nucleate very rapidly).

Most of the idocrase crystals observed in probe sections gave Na values of 0.1–0.2 percent; occasional larger crystals were found, and these exhibited the same low values for  $\text{Na}_2\text{O}$ . Atomic absorption analysis for Na in well-washed run products of the Na-containing gel ( $\text{Na}_2\text{O}=5\%$ ) have somewhat higher results (0.8%). However, analysis of a carefully separated crystal sample gave a value of 0.13 percent  $\text{Na}_2\text{O}$ .

Now that the idocrase stability field has been partially determined, we are investigating the best conditions for crystal growth. The sizes reported in Table 3 (optical parameters) are those of some larger crystals found in this continuing study. When large crystals have been produced of all types of idocrase synthesized (various cation substitutions), complete chemical investigations will be attempted, and the results presented in a later paper.

#### OPTICAL PARAMETERS

Indices of refraction were determined in Na light, and corrected to  $25^\circ\text{C}$ , using Cargille Series M and Schillaber's high precision high-index oils. All oils were calibrated with a Leitz-Jelley Refractometer before use, and when a match was found between oil and refractive index of a sample, the oil was checked with the refractometer. The estimated accuracy ( $\pm 0.003$ ) is limited chiefly by the small size of many of the crystals examined. A fresh index oil, calibrated by Cargille with high accuracy, was measured periodically to check the precision of the experimental techniques.

Several synthetic idocrase samples exhibited an extremely low birefringence, and might, for practical purposes, be considered isotropic. In such cases only one index could be determined within the experimental error, and is reported as a "mean index." Optic figures could not be obtained on most specimens, and sign of elongation is not reported where crystals did not exhibit distinctly elongated prisms.

Optical data, as well as comments on maximum idocrase crystal size, other phases observed, and approximate idocrase yield, are given in Table 3.

Table 3 (samples a–f, k and l) shows a progressive increase in refractive indices of the synthetic idocrase, in the following order:  $\text{Co} > \text{Cu} > \text{Ni} > \text{Mg}$ . This is due to Ni and Co replacing Mg, and Cu replacing Mg and, to some extent, Ca (see X-ray section); Mg idocrase with Ca, Al/Si and Al respectively replaced by Mn, Ti and  $\text{Fe}^{3+}$  (Table 3, samples h, g, and m) gave indices very slightly (but distinguishably) higher than the unsubstituted synthetic Mg idocrase.

The products obtained from sodium-containing starting materials gave markedly lower refractive indices (Table 3, samples i, j, k and l)

TABLE 3. RESULTS OF OPTICAL DETERMINATIONS<sup>a</sup>

SYNTHETIC IDOCRASE							
Sample	$\omega$	$\epsilon$	Birefr.	Elonga- tion	Max. X-sect. dimensions ( $\mu$ )	Approx. yield	Other phases identified
$\text{Ca}_{20}(\text{M})_4\text{Al}_8\text{Si}_{18}\text{O}_{68}(\text{OH})_8$ (Na-free)							
a) Mg	Mean: 1.696	1.701	0	—	4×60 (48 hrs.) 5×15 (5 days)	100%	
b) Ni	1.721	1.715	0.006	L. fast	30×80	50%	Wollastonite
c) Co	1.728	1.727	0.001	L. fast	40×60	70%	Meliilite
d) Cu	1.725	1.715	0.010	L. fast	12×35	90%	Wollastonite
$\text{Ca}_{19}(\text{M})_4\text{Al}_{10}\text{Si}_{17}\text{O}_{68}(\text{OH})_8$ (Na-free)							
e) Mg	1.701	1.699	0.002	L. fast	10×40	100%	
f) Ni	Mean: 1.723		0	—	1×1	100%	
g) Ti	1.715	1.710	0.005	L. fast	2×5	75%	Wollastonite
h) Mn	Mean: 1.713		0	—	5×15	60%	Meliilite, Garnet
$\text{Ca}_{19}(\text{M})_4\text{Al}_{10}\text{Si}_{17}\text{O}_{68}(\text{OH})_8$ (Na present in runs)							
i) Mg	Mean: 1.695		0	—	5×10	95%	
j) Ni	Mean: 1.703		0	—	1×2	60%	Diopside
k) Co	1.719	1.713	0.006	L. fast	6×20	70%	
l) Cu	Mean: 1.715		0	—	20×100	70%	Wollastonite
m) Mg-Fe'''	Mean: 1.715		0	—	4×18	80%	
NATURAL IDOCRASE (for composition see Table 4)							
Sample	$\omega$	$\epsilon$	Birefr.	<i>Xl. color</i>	<i>Locality</i>		
n)	1.705	1.697	0.008	Blue	Sauland, Norway (cyprine)		
o)	1.712	1.703	0.009	Brown	Sanford, Maine		
p)	1.722	1.713	0.009	Pale Green	Asbestos, Quebec		

<sup>a</sup> Where crystals were virtually isotropic (differences in index of refraction less than error in measurement,  $\pm 0.003$ ) a mean index has been reported. Additional phases are noted, where they were identifiable. Yield refers to idocrase crystals vs. amorphous products, and is a visual estimate. Approximate maximum size of idocrase crystals was determined with a micrometer ocular.

than those obtained in sodium-free runs (samples a-f). However, all measured refractive indices of the synthetic idocrase samples fall within the range observed in natural specimens. Those of three natural idocrases of known composition (Table 4, n, o and p) are given in Table 3 for comparison. Owing to the great complexity of idocrase chemical composition and the uncertainties in its formula, no further attempt to systematically correlate refractive indices with composition was made here.

TABLE 4. UNIT CELL DIMENSIONS OF SYNTHETIC AND NATURAL IDOCRASE. VALUES FOR SANFORD, MAINE AND ASBESTOS, QUEBEC ARE REPORTED IN THE COMPARATIVE STUDY GIVEN IN TABLE 5.

Synthetic Idocrase Gel composition	$a$ (Å)	$c$ (Å)	$V_{ol}$ (Å <sup>3</sup> )	$T$ (°C)	$P$ (kbar)	Duration (days)	Starting Materials
a) $Ca_{20}Mg_2Al_8Si_{18}O_{88}(OH)_8 \cdot nH_2O$	15.579(2)	11.837(3)	2873.2(7)	660	1.5	5	Ca(OH) <sub>2</sub> , Mg(OH) <sub>2</sub> and Al-silicate gel.
b) $Ca_{20}Ni_4Al_8Si_{18}O_{88}(OH)_8 \cdot nH_2O$	15.560(3)	11.809(4)	2859.1(1.0)	680	1.8	2	Ca(OH) <sub>2</sub> , NiCO <sub>3</sub> and Al-silicate gel.
c) $Ca_{20}CoAl_8Si_{18}O_{88}(OH)_8 \cdot nH_2O$	15.585(3)	11.815(3)	2869.5(9)	600	2.0	1	Ca(OH) <sub>2</sub> , CoCO <sub>3</sub> and Al-silicate gel.
d) $Ca_{20}CuAl_8Si_{18}O_{88}(OH)_8 \cdot nH_2O$	15.533(4)	11.757(3)	2836.7(1.2)	575	2.0	3	Ca(OH) <sub>2</sub> , CuCO <sub>3</sub> ·Cu(OH) <sub>2</sub> and Al-silicate gel.
e) $Ca_{10}Mg_2Al_8Si_{17}O_{86}(OH)_8 \cdot nH_2O$	15.600(1)	11.829(2)	2878.6(6)	650	1.5	7	Ca(OH) <sub>2</sub> , Mg(OH) <sub>2</sub> and Al-silicate gel.
f) $Ca_{10}Ni_4Al_8Si_{17}O_{86}(OH)_8 \cdot nH_2O$	15.575(3)	11.809(4)	2864.6(1.2)	650	1.5	2	Ca(OH) <sub>2</sub> , NiCO <sub>3</sub> and Al-silicate gel.
g) $Ca_{10}Mg_2TiAl_8Si_{17}O_{86}(OH)_8 \cdot nH_2O$	15.606(5)	11.829(3)	2880.9(7)	685	1.8	2	Ca(OH) <sub>2</sub> , Mg(OH) <sub>2</sub> and Al-Ti silicate gel.
h) $Ca_{10}Mn_2Mg_2Al_8Si_{17}O_{86}(OH)_8 \cdot nH_2O$	15.579(3)	11.806(7)	2865.6(1.7)	685	1.8	2	Ca(OH) <sub>2</sub> , Mg(OH) <sub>2</sub> and MnCO <sub>3</sub> and Al-silicate gel.
(Following compounds synthesized with 5% Na <sub>2</sub> O in capsules)							
i) $Ca_{10}Mg_2Al_8Si_{17}O_{86}(OH)_8 \cdot nH_2O$	15.632(4)	11.854(3)	2896.4(1.4)	550	2.0	2	Coprecipitated gel in NaOH
j) $Ca_{10}Ni_4Al_8Si_{17}O_{86}(OH)_8 \cdot nH_2O$	15.593(2)	11.821(3)	2874.2(8)	555	2.0	7	Coprecipitated gel in NaOH.
k) $Ca_{10}Co_2Al_8Si_{17}O_{86}(OH)_8 \cdot nH_2O$	15.562(2)	11.789(3)	2855.1(1.0)	555	2.0	7	Coprecipitated gel in NaOH.
l) $Ca_{10}Cu_2Al_8Si_{17}O_{86}(OH)_8 \cdot nH_2O$	15.553(2)	11.812(4)	2857.2(1.5)	555	2.0	7	Coprecipitated gel in NaOH.
m) $Ca_{10}Mg_2Fe^2+Al_8Si_{17}O_{86}(OH)_8 \cdot nH_2O$	15.605(3)	11.852(3)	2886.3(9.9)	550	2.0	2	Coprecipitated gel in NaOH.
<i>Natural Idocrase</i>							
Sample locality (ref.)	$a$ (Å)	$c$ (Å)	$V_{ol}$ (Å <sup>3</sup> )	Formula			
n) Saultand, Norway (cyprine) <sup>a,b</sup> (Neuman and Svinndal, 1955)	15.500(1)	11.773(1)	2840.2(3)	$Ca_{17.2}Ca_{10.2}Na_{0.1}K_{0.1}Mg_{10.6}Fe^{2+}_{10.1}Fe^{3+}_{0.2}Al_{10.7}Ti_{1.0}Si_{17.6}O_{86}(OH)_8(F)_8$ (analyst B, Brunu)			
o) Sanford, Maine <sup>b</sup> (present study)	15.533(4)	11.777(1)	2841.81(8)	$Ca_{18.2}Na_{0.2}Fe_{1.3}Mg_{10.6}Al_{10.6}Si_{17.6}O_{86}(OH)_8$ (microprobe, J. Aren)			
p) Asbestos, Quebec (present study)	15.523(1)	11.817(1)	2847.4(2)	$Mn_{0.1}Ca_{18.1}Na_{0.1}Mg_{10.6}Fe^{2+}_{10.1}Fe^{3+}_{0.2}Al_{10.6}Si_{17.6}O_{86}(OH)_8$ (analyst J. Ito)			

<sup>a</sup> Cell size determined in this study

<sup>b</sup> Chemical and optical data are taken from the indicated literature.

## X-RAY STUDY

*Experimental.* Lattice parameters of selected natural and synthetic idocrase samples were determined by least-squares analysis of X-ray powder diffractometer data, using a modified version of the digital computer program of Burnham (1962). Each sample selected for analysis was ground in an agate mortar with the internal standard (see below) and deposited on a glass slide with a collodion-amyl acetate mixture. The collodion used as a binder gave a permanent powder mount. Using a Phillips wide-range goniometer (model 42201) with Ni-filtered Cu radiation, scans were made at  $0.25^\circ \text{ min}^{-1}$  in the range  $25^\circ$ – $85^\circ$  ( $2\theta$ ) with a chart speed of one inch per minute. In several cases the same mount was rerun, and the two charts were measured and refined independently, as a check on the precision of the technique. Where this was done, the results differed by  $0.002 \text{ \AA}$  or less. Angles were measured with an estimated error of  $0.005^\circ$  in  $2\theta$ , and in most cases convergence to the final values for  $a$  and  $c$  occurred after only two least-squares cycles.

The refined lattice parameters given in Table 4 are referred to the semiconductor grade silicon (99.999% Si; 0.003 ppm B) used as an internal standard. The silicon was provided by M. Kastner and D. Waldbaum, Department of Geological Sciences, Harvard University, and is the same material used in Waldbaum's (1966) study of alkali feldspars. The lattice parameter  $[a]$  of this material was assigned the value  $5.43054 \pm 0.00017 \text{ \AA}$  at  $25^\circ\text{C}$  (Parrish, 1960). The X-ray wavelengths used in the refinements are  $\text{CuK}\alpha_1 = 1.54051$ ,  $\text{CuK}\alpha_2 = 1.54433 \text{ \AA}$ .

All diffractometer charts were indexed with the aid of "standard charts," prepared with idocrase from Asbestos, Quebec, and Sanford, Maine. The cell dimensions of these crystals had been determined with back-reflection Weissenberg photographs, and a complete set of possible  $d$ -values calculated. Three-dimensional structure factor data were available for both crystals, having been collected for crystal structure determination and refinement (J. Arem, in progress). An unambiguously indexed powder pattern for synthetic Mg idocrase is given in Table 6. The chart for idocrase from Asbestos, Quebec, was mea-

TABLE 5. ACCURACY AND PRECISION OF CELL DETERMINATIONS\*

Specimen	PRECISION WEISSENBERG PHOTOS			
	Independent Observations	$a$	$c$	volume
Sanford, Maine	91	15.53334(15)	11.77783(18)	2841.81(8)
Asbestos, Quebec	109	15.52315(38)	11.81665(23)	2847.44(18)
DIFFRACTOMETER DATA				
Asbestos, Quebec	56	15.52191(58)	11.81632(81)	2846.90(19)
All (Chart) data				
Partial Data	37	15.52135(50)	11.81750(94)	2846.98(20)
(best lines)				
Partial Data	20	15.52340(131)	11.81467(159)	2847.05(51)

\* Results of back-reflection Weissenberg photographs, refined by least-squares, compared with refinements based on diffractometer chart measurements. Comparison of results obtained from diffractometer data, using all indexed lines versus partial data (both high and low quality peaks).

TABLE 6. X-RAY POWDER DATA FOR SYNTHETIC Mg-IDOCRASE<sup>a</sup>

<i>hkl</i>	<i>I/I</i> <sub>0</sub>	<i>d</i> (obs.)	<i>d</i> (calc.)	<i>hkl</i>	<i>I/I</i> <sub>0</sub>	<i>d</i> (obs.)	<i>d</i> (calc.)
110	7	10.99	11.031	641	10	2.128	2.128
101	5	9.42	9.426	623	7	2.091	2.091
111	5	8.03	8.067	712	5	2.067	2.067
201	7	6.50	6.511	730	5	2.047	2.048
002	5	5.91	5.914	642	2	2.031	2.032
220	3	5.51	5.515	731	2	2.017	2.018
202	5	4.71	4.713	633	5	2.003	2.003
212	3	4.51	4.511	651	2	1.969	1.970
222	5	4.03	4.033	515	1	1.871	1.872
420	10	3.48	3.488	316	1	1.831	1.831
402	4	3.254	3.256	822	1	1.802	1.802
510	10	3.058	3.059	714	7	1.768	1.768
431	5	3.020	3.017	406	6	1.759	1.759
004	20	2.957	2.957	910	5	1.721	1.723
323	3	2.915	2.914	436	10	1.667	1.667
440	100	2.758	2.758	804	22	1.628	1.628
530	5	2.675	2.675	770	5	1.576	1.576
522	55	2.600	2.602	664	10	1.562	1.561
314	2	2.538	2.536	844	5	1.502	1.502
442	3	2.499	2.499	008	1	1.478	1.479
620	25	2.464	2.466	774	3	1.391	1.391
541	1	2.386	2.386	954	3	1.348	1.349
602	3	2.380	2.386	1044	3	1.301	1.301
404	4	2.355	2.356	926	2	1.284	1.284
414	4	2.331	2.330				
334	2	2.304	2.304				
631	4	2.281	2.282				
710	3	2.206	2.206				
701	1	2.190	2.190				
711	3	2.168	2.169				

<sup>a</sup> Measurements made on chart prepared for cell size determination. Idocrase used is: Ca<sub>19</sub>Mg<sub>4</sub>Al<sub>10</sub>Si<sub>17</sub>O<sub>68</sub>(OH)<sub>8</sub>, synthesized at 690°C., 1.5 kbar. Cell (as refined) for *d*(calc.): *a* = 15.600 (1) *c* = 11.829 (2) Cu radiation (Ni-filtered) K $\alpha_1$  = 1.54051 K $\alpha_2$  = 1.54178. All *d*-values calculated with computer program (IBM 7094) and are given in Ångstroms.

sured (and cell dimensions refined by least-squares technique) in the same way as those for all the synthetic crystals. The results compare quite favorably with the high-precision Weissenberg values (Table 5). This independent check provides confidence in the accuracy of the cell dimensions reported here, since the least-squares precision is only representative of the internal consistency, and does not reveal anything of systematic errors. We estimate the accuracy of the cell dimensions to be  $\pm 0.002$  Å.

Table 5 also shows the effects of reducing the number of observations processed in the refinement of cell dimensions by least-squares. It is significant that the same values (within the estimated error) were obtained using all the data, and when the highest quality or lower quality lines were run alone. With only two refinable parameters (*a* and *c*), a small

number of independent observations (diffractometer peak measurements of planes with general indices) can converge to an accurate result.

*Results.* Although the unit cell dimensions of all our synthetic idocrase fall within the known range for natural specimens (Deer, Howie and Zussman, 1962), the synthetic Mg-idocrase has an appreciably larger cell volume and cell-edge  $a$  than the natural samples measured in this study (Table 4, specimens n, o and p). The chemical compositions of these specimens (calculated as formulas in Table 4, n, o and p) is very complex, and they all contain both ferric and ferrous iron. We were thus unable to clearly relate cell-size variations to differences in composition.

A possible explanation for the smaller unit cell dimensions of natural idocrase as compared to the synthetic idocrase is the effect of fluorine substitution, or of cation or anion site deficiencies, including partial dehydroxylation in the natural mineral. Synthetic products were crystallized under somewhat favorable  $P$ - $T$ - $X$  conditions, in a water-saturated environment and with simpler chemical components as starting materials. Natural idocrase probably forms under less suitable conditions, in which site deficiencies seem more likely.

The unit cell dimensions for the idocrase crystallized in an alkaline environment from the same starting composition,  $\text{Ca}_{19}\text{Mg}_4\text{Al}_{10}\text{Si}_{17}\text{O}_{68}(\text{OH})_8$  (Table 4, i) ( $a = 15.632 \text{ \AA}$ ;  $c = 11.854 \text{ \AA}$ ) are appreciably larger than those for idocrase crystallized in an alkali-free environment ( $a = 15.600 \text{ \AA}$ ;  $c = 11.829 \text{ \AA}$ ), (Table 4, e). Appreciable Na substitution in Ca sites was first suspected, but electron probe analysis for the idocrase crystals obtained in the sodium-containing system gave fairly low values for sodium ( $\text{Na}_2\text{O} = 0.1\text{--}0.2\%$ ).<sup>1</sup> The amounts do not seem sufficiently large to affect either the unit cell dimensions or the optical properties. It is possible that in the idocrase formed under such conditions a small amount of non-ionic (interstitial) water has been incorporated. Infrared analysis did not show an appreciable difference in OH absorption intensity, measured at  $3650 \text{ cm}^{-1}$ .

Very slight differences in the unit cell dimensions were observed between the idocrase obtained from two different gel compositions in a sodium-free environment (see Table 4, samples a and e). Since substitutions in idocrase could take place in more than one site, these small differences are left unexplained.

Among various divalent cations investigated in replacement studies,

<sup>1</sup> Wet analysis (atomic absorption spectrophotometry) gave a value of 0.13%  $\text{Na}_2\text{O}$  for Mg idocrase single crystal made in an alkaline environment, and of 0.8%  $\text{Na}_2\text{O}$  for bulk Mg-idocrase sample from the Na-containing (5%) gel. Probe analysis may be slightly low due to Na loss in electron beam.

only  $\text{Cu}^{2+}$ ,  $\text{Co}^{2+}$  and  $\text{Ni}^{2+}$  analogs were obtained in both alkali-containing and alkali-free environments. Partial replacements by  $\text{Mn}^{2+}$ ,  $\text{Fe}^{3+}$ , and  $\text{Ti}^{4+}$  were also achieved. The optics and cell data are given in Tables 3 and 4. The cell dimensions of all the synthetic idocrase samples examined fall close to the range of natural specimens (Table 4, o and p). Synthetic Cu- (Table 4, d and l) and natural Cu-bearing idocrase (Table 4, n, cyprine) (Neumann and Svinndal, 1955) have the smallest observed cell size, and Mg-idocrase (Table 4, a, e and i) has the largest. This might at first seem surprising, since ionic radius values<sup>1</sup> would lead to prediction of the reverse trend. A likely explanation for the observed behavior is a mechanism of replacement involving  $M$ —Ca (where  $M$  is Cu, Co, Ni, Mg or Mn) rather than  $M$ —Mg, in the idocrase structure. With this assumption, one would predict the observed trend, since Cu is closest in size to Ca, though smaller. This would enable more Cu to replace Ca than would Co, Ni, or Mg, with correspondingly greater relative decrease in cell size. Synthetic Mg-idocrase, with little Ca-replacement, is closest in cell size to most natural idocrase specimens.

Support for the inferred larger Cu-Ca replacement comes from the observation of wollastonite as an additional phase in the Cu runs. The starting composition of all runs was adjusted to produce a single-phase idocrase as a product. The presence of a second Ca-bearing phase clearly indicates a Ca deficit in the idocrase, which might be the result of Cu replacement.

The smaller unit cell dimensions for the  $\text{Co}^{2+}$  (Table 4, c and k) analog, compared to those for the  $\text{Mg}^{2+}$  end member, also cannot be explained only by replacements in Mg (6-coordinated) sites, because the conventionally accepted ionic radius for  $\text{Co}^{2+}$  (0.735 Å) is larger than that of  $\text{Mg}^{2+}$ . It is likely that  $\text{Co}^{2+}$  also replaces  $\text{Ca}^{2+}$  in 8-coordinated sites. The effect of partial replacement of the larger Ca ions by Co reduces the cell size, as is the case with  $\text{Cu}^{2+}$ .

The differences between the unit cell dimensions of the  $\text{Mg}^{2+}$  and  $\text{Ni}^{2+}$  end-members (Table 4, b, f and j) are, however, consistent with those between the ionic radii of these elements ( $\text{Ni}^{2+}=0.700$  Å,  $\text{Mg}^{2+}=0.720$  Å). This suggests that nearly all the  $\text{Ni}^{2+}$  ions are restricted to 6-coordinated Mg sites. No natural counterparts for the  $\text{Ni}^{2+}$  and  $\text{Co}^{2+}$  analogs have been found.

Idocrase containing up to 3 weight percent ferrous oxide has been described (Meen, 1939). Divalent Fe (radius=0.77 Å) may replace to some extent both Mg (6-coordinated) and Ca (8-coordinated). However,

<sup>1</sup> Ionic radii refer to the values recently given by Shannon and Prewitt (1969).

even an intermediate (Fe<sup>2+</sup>-Mg)-idocrase was not obtained because of the large stability range of Fe<sup>3+</sup>-rich grossular. Idocrase whose iron is all divalent may crystallize in a strongly reducing environment in which andradite breaks down.

Ferric iron has almost always been found in idocrase, but in amounts smaller than several weight percent. The results of our experiments showed that less than one-tenth of the Al sites of Mg-idocrase can be filled by Fe<sup>3+</sup>. With further increase of ferric iron, idocrase begins to break down to an Fe<sup>3+</sup>-rich grossular. The unit cell dimensions of ferric-iron-containing idocrase<sup>1</sup> (synthetic, Table 4, m) did not show an appreciable increase, as would be expected from replacement of Al<sup>3+</sup> by Fe<sup>3+</sup>. Some of the Fe<sup>3+</sup> ions may replace the larger Mg<sup>2+</sup> ions, thus compensating for the effects of ferric iron replacing Al, with charge balance possibly effected by partial dehydroxylation or cation deficiency.

Divalent manganese ions are sometimes found in naturally-occurring idocrase, causing a pink color. Partial introduction of Mn into synthetic idocrase was achieved from a mixture of the following composition: Ca<sub>18</sub>Mn<sub>2</sub>Mg<sub>3</sub>Al<sub>10</sub>Si<sub>17</sub>O<sub>68</sub>(OH)<sub>8</sub>·*n*H<sub>2</sub>O. An appreciable decrease in unit cell dimensions of the Mn-idocrase (Table 4, h) from those of the magnesian equivalent: Ca<sub>19</sub>Mg<sub>4</sub>Al<sub>10</sub>Si<sub>17</sub>O<sub>68</sub>(OH)<sub>8</sub> indicates that most of the Mn<sup>2+</sup> enters Ca sites, and not Mg sites. This conclusion is not considered definitive because the material has not been analyzed. Neither Zn<sup>2+</sup> nor Be<sup>2+</sup> analogs (Hurlbut, 1955) have been synthesized. Under the present experimental conditions, garnet and Zn- or Be-melilite always formed instead.

A tetravalent element often found in natural idocrase specimens is Ti. The role of Ti in the idocrase structure is not yet understood, but the mechanism of titanium replacement in idocrase may be similar to that in schorlomite (Ti-garnet). Most of the titanium may occupy 6-coordinated sites instead of 4-coordinated sites (Dowty, E. and Mark, R., 1968), with valency compensation effected by Al↔Si and Ti↔Al substitutions. At any rate, large amounts of titanium do not seem able to enter the idocrase structure. A nearly single-phase idocrase was obtained from a mixture corresponding to Ca<sub>19</sub>Mg<sub>4</sub>TiAl<sub>10</sub>Si<sub>16</sub>O<sub>68</sub>(OH)<sub>8</sub>·*n*H<sub>2</sub>O (Table 4, g). The unit cell dimensions showed a marked increase compared to those of the pure Mg end-member of the corresponding composition. Further increase of Ti<sup>4+</sup> in the above compositions resulted in the appearance of a second phase, such as sphene and/or perovskite.

Sodium has been noted (up to 0.8%) in the analyses of naturally-occurring idocrase. It is obvious that some sodium replaces calcium with other valency compensations, but the amount of the replacement

<sup>1</sup> Calculated weight percent Fe<sub>2</sub>O<sub>3</sub>=2.86%.

appears to be rather limited. Runs with starting compositions of  $\text{Ca}_{18}\text{NaMg}_4\text{Al}_9\text{Si}_{18}\text{O}_{68}(\text{OH})_8$  or  $\text{Ca}_{18}\text{NaMg}_2\text{Al}_{11}\text{Si}_{17}\text{O}_{68}(\text{OH})_8$  did not crystallize to a single-phase idocrase at 650°C an 1.5 kbar, but the former produced a more nearly monophasic product. Some titanium-bearing idocrase found in nepheline syenite (Inoue and Miyashiro, 1951) is also rich in sodium, suggesting that a sodium-titanium coupled substitution may be operative (e.g.,  $\text{Ca}_{18}\text{NaMg}_4\text{Al}_9\text{TiSi}_{17}\text{O}_{68}(\text{OH})_8$ ).

Minor amounts of chromium were found in idocrase associated with chromite ore from the Ural Mountains (Kurbatov, 1922). Sr and Ga are also known as trace elements in some idocrases. Attempts at major substitution of the above elements failed. Rare earth and Ge replacements are left for further studies. Fluorine-bearing idocrase is known in nature, but its synthesis has not been achieved so far. If pure fluoro-idocrase does exist, it might be grown at high temperatures, probably by using a flux.

#### KINETICS

A rigorous study of reaction kinetics would require quantitative data on the phases reacting and on those produced. Although such detailed work has not been attempted in the present study, qualitative trends are still quite meaningful. We believe that the diagrams given here offer a close approximation to the scheme of chemical interaction, and are useful in understanding the complex processes involved.

(1) The rate of hydrothermal crystallization of idocrase is temperature pressure, and composition dependent. Experiments under three different sets of conditions (660°C, 3 kbar; 660°C, 1.5 kbar; 550°C, 1.5 kbar) were performed, using a sodium-free gel having the composition  $\text{Ca}_{19}\text{Mg}_4\text{Al}_{10}\text{Si}_{17}\text{O}_{68}(\text{OH})_8 \cdot n\text{H}_2\text{O}$ . In analyzing run products by X-ray diffractometry, the scale factor was set in such manner that the highest diffraction peaks of idocrase (440) and grossular (420) would approximately reach the limit of the recording chart scale when samples were pure single crystalline phases. Then relative peak heights were directly plotted against run duration (using a logarithmic scale). This duration is the period between the time when the sample reached the reaction temperature and the instant of quenching. Fairly smooth curves were thus obtained (Fig. 4). Minute quantities of other metastable phases such as calcite, melilite, wollastonite, monticellite and diopside were detected, but not plotted.

From the results, it is clear that the reaction rates are increased and induction times are shortened by rising temperatures and pressures, although the general scheme of the whole reaction series remains unaffected. The reaction series found here may be written as follows:

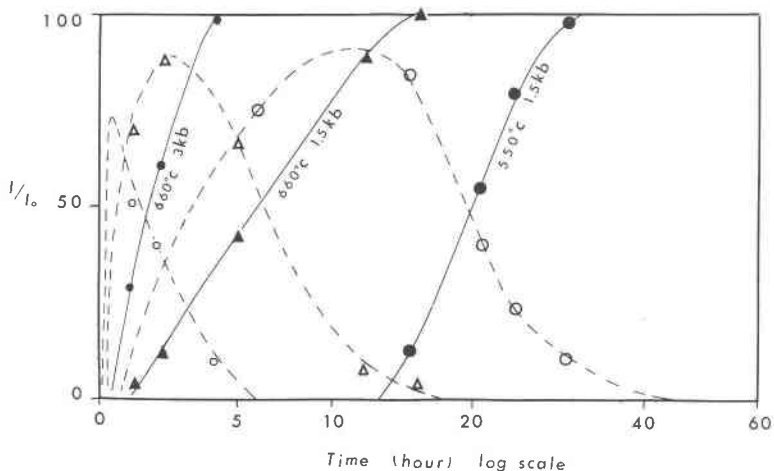


FIG. 4. Tentative kinetics diagram for idocrase crystallization from a gel of composition  $\text{Ca}_{19}\text{Mg}_4\text{Al}_{10}\text{Si}_{17}\text{O}_{68}(\text{OH})_8 \cdot n\text{H}_2\text{O}$ . Solid circles and triangles on black line=idocrase. Large circles represent runs at  $550^\circ\text{C}$ , 1.5 kbar. Triangles represent runs at  $660^\circ\text{C}$ , 1.5 kbar. Small circles represent runs at  $660^\circ\text{C}$ , 3 kbar. Small open circles and open triangles on dotted line=metastable garnet. Abscissa is a  $\log_{10}$  scale; ordinate is relative peak intensity.

Amorphous Ca, Mg and Al hydrous silicates+hydrogrossular-hydro-pyrope ( $a = 12.43 \text{ \AA}$ )→slightly hydrated metastable grossular-pyrope ( $a = 11.88 \text{ \AA}$ )→Mg-idocrase. The presence of hydropyrope was suggested by Christie (1961). We also suspect that Mg atoms may be involved with all the idocrase-forming reactions, probably entering in distorted co-ordination polyhedra of a metastable garnet-like structure. However, under moderate pressures, Mg atoms cannot stably occupy the 8-co-ordinated sites in the grossular structure. Idocrase then forms, in which Mg atoms find stable 6-coordinated sites. Furthermore, rapid recrystallization of idocrase from the metastable garnet indicates that there may be only a small energy difference involved in the process. This is consistent with the great similarity between the two structures.

(2) Starting gels (sodium-free) having different cation ratios showed significant differences in rate of nucleation and growth of idocrase, and also showed rather interesting varieties of processes. Kinetics of nine selected sodium-free gels having compositions within the idocrase-pre-dominant regions were investigated at  $650^\circ\text{C}$ , 1.5 kbar in some detail, for the first 20 hours. These nine compounds were derived by permuting combinations of  $x$  and  $y$  in the formula:



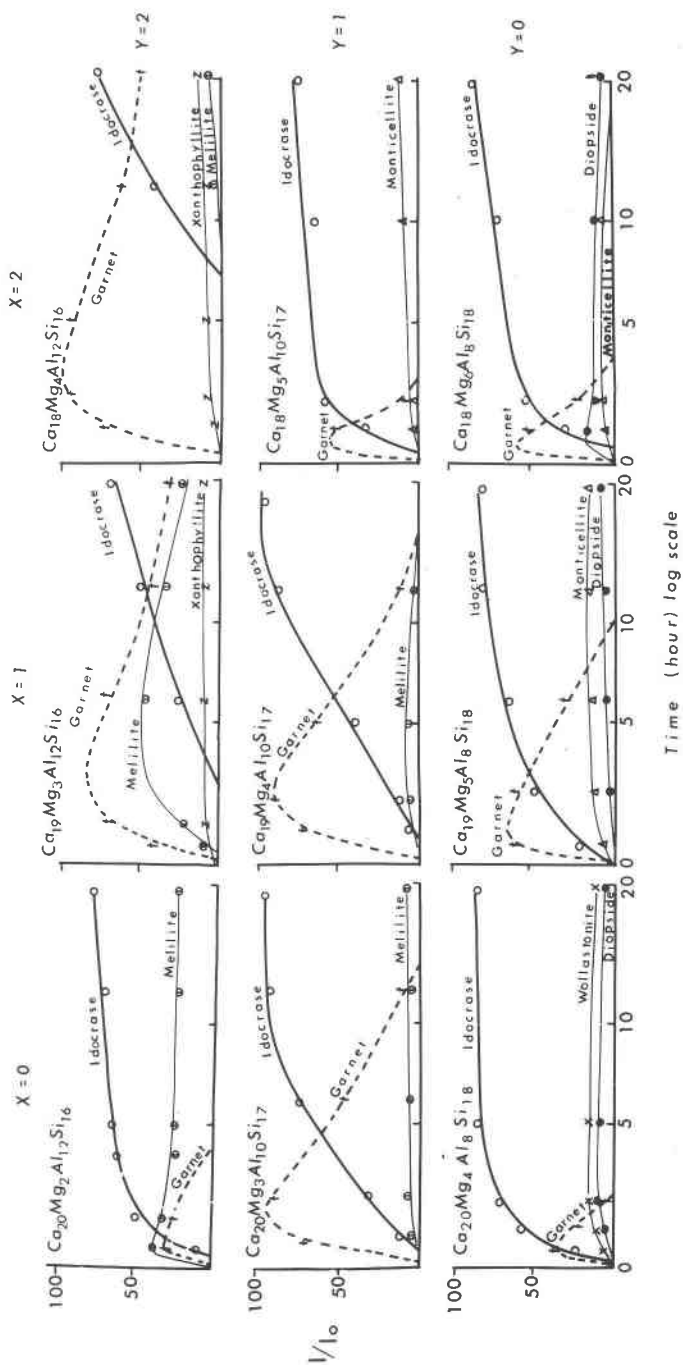
where  $x=0, 1$  and  $2$ , and  $y=0, 1$  and  $2$ . The process and rate of crystallization of compounds of these compositions were significantly different, and are given graphically in Fig. 5. These kinetic diagrams are arranged according to the numbers  $x$  and  $y$  used to derive the different compositions from the working formula here proposed. The parameter  $y$  increases from  $0$  to  $2$  vertically and  $x$  increases from  $0$  to  $2$  horizontally. The compositional trend of this arrangement coincides with that of our *ACF* diagram given in the previous section (Fig. 2). In other words, Si and Mg decrease upwards, with concomitant replacement by two Al in the formula, and only  $\text{Ca} \rightleftharpoons \text{Mg}$  replacement takes place horizontally, the Al:Si ratio remaining constant.

In the kinetics diagram of each composition, the logarithm of the experimental run time (in hours) is plotted along the abscissa, with the ordinate displaying the relative proportions of various phases produced in each run. In all cases the latter was equated with peak heights on diffractometer charts, with the following peaks used: idocrase, 440; grossular, 420; melilite, 211; wollastonite, 202; diopside, 311; monticellite, 111; xanthophyllite, 200. The plots for idocrase, grossular and melilite are scaled so that a synthetic monophase specimen would give a value of 100 percent along the ordinate. The other phases have not been so scaled and their abundance has, if anything, been exaggerated. Our study confirmed that idocrase solid solution lies in the vicinity of the compositions given with  $0 < x < 1.5$  and  $0.2 < y < 1.2$  or near to the formulas:



These gel compositions gave remarkably simple reaction kinetics, consisting mostly of garnet, idocrase and a very small amount of metastable melilite. These experiments also showed that the appearances of the metastable phases largely depend on the stability relations of adjacent phases in the quaternary system. A nearly stoichiometric composition does not necessarily produce idocrase with the fastest rate of reaction. In the compositions supposedly containing excess Ca or Mg, nucleation of idocrase is induced during the early stages of heating, probably due to the active hydroxyl ions in a stronger alkaline environment created by excess Ca or Mg. On the other hand, excess Al appears to introduce an appreciable induction period during which no idocrase is observed.

Some of the results of our experiments are best seen in terms of the *ACF* diagram (Fig. 2). Although grossular plots (in projection) along the A-C join, its persistent and abundant appearance to the right (Mg-Al side) of the idocrase compositional field indicates a broad stability field



within the tetrahedron *A-C-F-SiO<sub>2</sub>* (Fig. 3). Furthermore, unit cell measurements of melilite appearing in our experiments show them to be gehlenite-rich. We can thus explain the observed persistence of melilite in runs whose starting composition lay on the alumina-rich portion of the assumed idocrase stability field.

(3) The effects of using different starting materials in a multi-component system are rather complex. Not only the nature of the starting materials, but also a small difference in the ratio of the components changes the whole scheme of observed reactions. Furthermore, all the reaction series are temperature and pressure dependent. It is no wonder that the literature on the synthesis of complex silicates so far contains remarkably little information on reaction kinetics. Although it is clear that many actual reactions are in practice determined by kinetic rather than stability relationships, we also realize that the present study on the kinetics of idocrase is but rudimentary. We have, however, become convinced of the basic difficulties involved, and present here three typical reactions from the most commonly used starting materials employed to obtain crystalline idocrase.

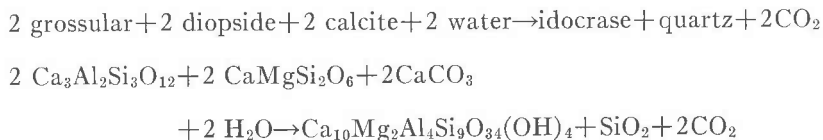
*Reaction in a Strongly Alkaline Environment.* (pH of residual liquid = 9.5). A very fast reaction was effected by using a coprecipitated alkali-containing gel (Fig. 6a). This gel is of the same composition as that used for pressure-temperature stability studies described in the previous section [*i.e.*  $\text{Ca}_{19}\text{Mg}_4\text{Al}_{10}\text{Si}_{17}\text{O}_{68}(\text{OH})_8$ ]. At 550°C under 2 kbar (water) pressure, almost all of the gel was converted within 4 hours to idocrase, probably a hydrated variety with larger unit cell dimensions. Small amounts of metastable garnet and melilite were observed at an early stage. Insignificant amounts of calcite, which were not plotted, persisted throughout, probably having formed during gel preparation. The rate of the reaction seemed to be increased not only by the great reactivity of the coprecipitated gel, but also by the high concentration of hydroxyl ions (NaOH) in the system, because idocrase contains (OH) or halogen as an essential structural component.

---

←

Fig. 5. Kinetics diagram, at 650°C, 1.5 kbar, for nine compounds derived from the general formula for idocrase presented in this study:  $\text{Ca}_{18}(\text{Ca}_{2-x}\text{Mg}_x)\text{Mg}_2(\text{Mg}_{2-y}\text{Al}_y)\text{Al}_8(\text{Al}_y\text{Si}_{2-y})\text{Si}_{16}\text{O}_{68}(\text{OH})_8$ , changing combinations of *x* and *y* in the formula. In the diagram, *x* takes the values 0, 1 and 2 and *y*=0, 1 and 2. The composition of the starting material is given above each kinetics diagram.

*Reaction of (Mg, Al) Hydro-silicate Gels and Calcite.* This starting material was prepared by mixing  $\text{Al}(\text{OH})_3$ ,  $\text{Mg}(\text{OH})_2$  and  $\text{CaCO}_3$  in Na-free silicic acid solution to achieve the desired composition for crystallizing  $\text{Ca}_{19}\text{Mg}_4\text{Al}_{10}\text{Si}_{17}\text{O}_{68}(\text{OH})_8$ . At  $690^\circ\text{C}$  and 1.9 kbar a large amount of calcite decomposes quickly in the first  $\frac{1}{2}$  hour to form metastable diopside and garnet. These metastable phases react with the remaining calcite to form a single-phase idocrase within 48 hours (Fig. 6b). The rate of the reaction is considerably slower than any reactions using gel or hydroxide starting mixtures. The size of individual crystals is much larger because of limited nucleation. The above reaction can be written ideally as follows:



*Reaction of Hydroxide Mixtures.* Idocrase can also be hydrothermally synthesized using a precise mixture of hydroxides or oxides. The rate of the reactions is approximately half of that with the gels. If starting hydroxides are calcined at  $1,000^\circ\text{C}$  for 24 hours, or partly replaced by carbonates, the rate can be greatly retarded. Idocrase of the composition  $\text{Ca}_{19}\text{Mg}_4\text{Al}_{10}\text{Si}_{17}\text{O}_{68}(\text{OH})_8$ , accompanied by minute amounts of monticellite, was crystallized at  $650^\circ\text{C}$  under 1.5 kbar for 24 hours, as shown in Fig. 6c. The metastable formation of a large amount of melilite is typical of this crystallization series. Small amounts of garnet appeared metastably, but disappeared much earlier than melilite. All other experiments with this composition, using oxides or hydroxides, followed similar patterns. However, if the ratio of the hydroxide mixture was changed to  $\text{Ca}_{20}\text{Mg}_4\text{Al}_8\text{Si}_{18}\text{O}_{69}(\text{OH})_8$ , even under the same conditions, melilite no longer appeared as a metastable phase. Grossular and diopside became major metastable phases, and the crystallization of idocrase was completed in about 12 hours at  $650^\circ\text{C}$  and 1.5 kbar.

#### DISCUSSION

The results of our phase syntheses clearly show that, despite a close similarity, idocrase and grossular are compositionally quite distinct. Some contrary suggestions have been made; for example, "the controlling factor as to which mineral will actually crystallize may be related to the presence or absence of fluorine or other volatile constituents" (Deer, Howie and Zussman, 1962) and that "the formation of idocrase closely depends on the presence of alkali a in hydrothermal environment"

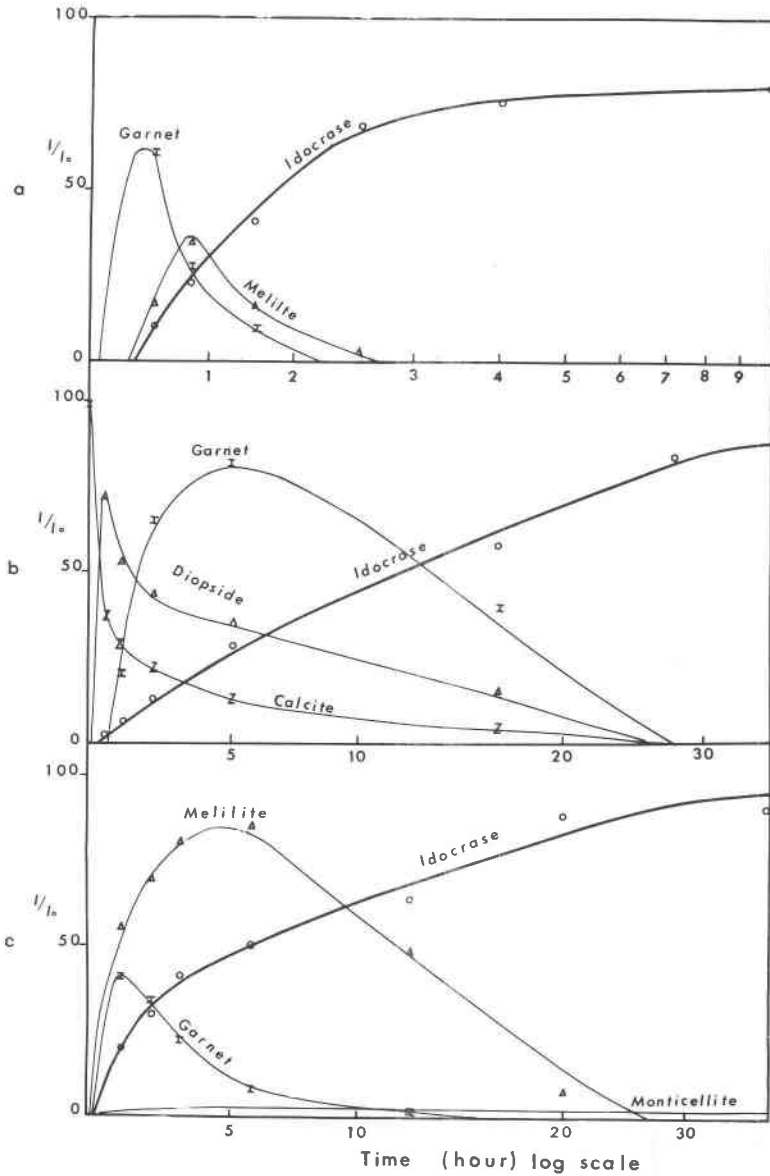


FIG. 6. Comparison of kinetics, demonstrating the effects of using different starting mixtures for crystallizing idocrase. Composition of gel used in the diagram:  $\text{Ca}_{19}\text{Mg}_4\text{-Al}_{10}\text{Si}_{17}\text{O}_{88}(\text{OH})_3 \cdot n\text{H}_2\text{O}$ .

- Coprecipitated gel in strongly alkaline solution ( $550^\circ\text{C}$ , 1 kbar).
- $\text{CaCO}_3$ ,  $\text{Mg}(\text{OH})_2$  and aluminosilicate, precipitated together ( $690^\circ\text{C}$ , 1.9 kbar).
- $\text{Ca}(\text{OH})_2$ ,  $\text{Mg}(\text{OH})_2$ ,  $\text{Al}(\text{OH})_3 \cdot n\text{H}_2\text{O}$  and  $\text{H}_2\text{SiO}_3 \cdot n\text{H}_2\text{O}$  mixture ( $650^\circ\text{C}$ , 1.5 kbar).

(Cristophe-Michel-Lévy, 1960). These suggestions are not consistent with our results.

Our experimental results suggest that idocrase will break down to a low temperature assemblage, such as hydrogrossular-dipside-xonotlite, at temperatures below 400°C. Idocrase was not obtained, but rather the assemblage wollastonite-grossular-melilite at pressures below 250 bars (Figs. 1a and 1b). However, the stability ranges of both idocrase and grossular overlap considerably under moderate pressures (1.5 kbar, with  $P_{\text{Tot}} = P_{\text{H}_2\text{O}}$ ) and temperatures (450–650°C). Idocrase will not break down to grossular and other phases without further compositional changes under these conditions, or unless  $P_{\text{H}_2\text{O}}$  is drastically reduced.

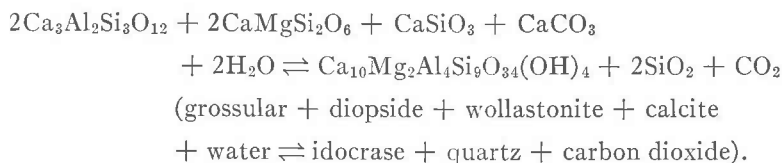
At Crestmore, California, the intrusion of a quartz-monzonite porphyry into a magnesian limestone (5% MgO) produced a thick silicate aureole. This aureole exhibits a well-defined sequence of mineral zones, described by C. Wayne Burnham (1959) as the monticellite, idocrase and garnet zones. Burnham concluded that the observed sequence of assemblages was the result of Si, Al and Fe metasomatism of the magnesian limestone. Burnham further indicated that the zonal arrangement was not due to gradations in  $P-T$  conditions, but rather to differences in the intensity of metasomatism, as reflected by the markedly different contents of silica, alumina, iron oxides and magnesia in the three zones. Our experimental results, which show the dominant effects of compositional changes versus water pressure-temperature variations, clearly support his conclusions. The experiments suggest that the three zones of silicate assemblages at Crestmore were formed at similar temperatures and total pressure (predominantly water pressure). The transition from a garnet to an idocrase zone might result from a rise in the activity of  $\text{H}_2\text{O}$  (with concomitant decrease in  $\text{CO}_2$  activity) as the composition of the vapor phase changed during metamorphism. It may be simpler to relate metasomatic grade to the  $(\text{Al}, \text{Fe}^{3+})/(\text{Mg}, \text{Fe}^{2+})$  ratio, because the Ca/Si ratio remains nearly constant within the aureole. Furthermore, the melilite found in the monticellite zone at Crestmore is gehlenite-rich, a fact which also is consistent with the composition of melilite ( $\text{Geh}_{30}\text{Ak}_{20}$ ) in our idocrase syntheses.

The process of metasomatism, involving alumina and silica, has produced so-called skarn zones in many localities throughout the world. The composition of the vapor phase during metasomatism (or perhaps in the period of cooling), notably the relative proportions of  $\text{H}_2\text{O}$  and  $\text{CO}_2$ , probably is very significant in determining whether or not idocrase forms at the expense of the rather stable grossular, because we have found that high  $\text{CO}_2$  activity favors Ca-garnet.

Grossular (or andradite) and diopside (or hedenbergite) are commonly

present as gangue in sulfide-skarn deposits. Here, idocrase seems to be conspicuously absent. The  $\text{CO}_2$  activity in a limestone undergoing metamorphism is undoubtedly high, and might allow for too small an activity of water for idocrase formation. The occasional presence of idocrase in scheelite-bearing skarns may be attributable to high concentrations of volatiles, such as F or OH. Sulfide deposition is often considered as due to oxidized solutions meeting a reducing environment, and much  $\text{Fe}^{3+}$  is frequently and initially present. Such conditions favor breakdown of idocrase to the more stable andradite and may account for the absence of idocrase in sulfide skarns. If an antipathetic relationship can be established between idocrase and skarn-sulfide deposits, it may be of significance in the search for ore deposits in limestone terranes

Minerals often found coexisting with idocrase in calcareous metamorphic rocks are grossular, diopside and wollastonite, and less frequently calcite, dolomite, quartz and monticellite. These mineral associations can be ideally illustrated by the following balanced chemical equation:



This equation includes all of the common naturally-occurring phases coexisting with idocrase, water and  $\text{CO}_2$ . It is clearly seen that idocrase stability increases with increasing water activity, and decreases as the activity of  $\text{CO}_2$  rises. Furthermore, one of the kinetic studies (Kinetics, section 3) using  $\text{CaCO}_3$  as a source material for CaO showed a process of idocrase crystallization (involving metastable phase formation) closely similar to that illustrated in the above equation.

In one of the best-known idocrase occurrences, that at Sanford, Maine, brown idocrase crystals were found embedded in massive quartz. Such an assemblage might easily be formed if the "idealized reaction" shown above were to go to completion.

The assemblage observed in nepheline-syenite has not been investigated in this study. It may be interesting to note that the stability range for idocrase expands considerably in the presence of alkali, towards the Al-rich part of the *ACF* diagram (Fig. 2). This fact is consistent with the finding by Inoue and Miyashiro (1951) that the idocrase in nepheline-syenite is richer in alumina than idocrase found in other types of occurrences.

The vuggy masses and free-growing nature of idocrase crystals from

asbestos deposits (as at Asbestos, Quebec, and Black Lake, Quebec) suggest formation at low pressures. Furthermore, the assemblages at these localities appear to have crystallized late in the paragenetic history of the surrounding rocks. The veins at Asbestos, Quebec, are characterized by a wealth of minerals apparently formed in a late stage of mineralization. This assemblage includes prehnite, calcite, diopside, uvarovite, albite, grossular, chlorite, xanthophyllite and sphene. Idocrase crystals found here are often intensely zoned. Some of them are doubly terminated and emerald-green at one end (due to Cr) but deep lilac at the other (due to Mn). This observation suggests that there were marked changes in the composition of the mineralizing solution. Ca in the above assemblage has apparently been derived from the breakdown of plagioclase in dike rocks, on encountering the cooler, water-rich environment of surrounding altered ultramafic rocks (De, 1961).

In summary, natural chemical variations in idocrase concern all the major constituents (Ca, Al, Mg, Si, O, OH) composing its structure, as well as replacements involving Be, B, F, Na, Ti, Cr, Mn,  $Fe^{2+}$ ,  $Fe^{3+}$ , Cu, Zn, Sn, Ce and rare earths. In synthetic studies we have produced Ni, Co and Cu analogs. The huge array of phases occurring in association with idocrase in nature can be attributed to: a) the broad range of chemical and physical conditions in which the mineral is stable, b) its central location within a rather complex chemical system, and c) the lack of complete equilibrium in many of the environments (such as metasomatized contact zones) in which it forms.

The kinetics of idocrase formation principally involves grossular and melilite. Grossular and idocrase are almost identical in composition, the apparently critical distinction being the presence of Mg and (OH) in idocrase. High  $CO_2$  activity favors the formation of grossular, probably due to a concomitant lowering of the activity of  $H_2O$  in the system. Idocrase formation is much more sensitive to compositional changes than to  $P_{H_2O}$ - $T$  variations.

Häuy's (1797) name "idocrase," meaning "mixed species," has proved to be prophetic. After 170 years, much still remains to be discovered about this enigmatic mineral.

#### ACKNOWLEDGEMENT

We wish to thank Professor Clifford Frondel for his interest and support. Thanks are also due to Professors J. B. Thompson, Charles W. Burnham and J. F. Hays, and to Dr. D. R. Waldbaum for critically reading the manuscript and offering valuable suggestions. We are also indebted to H. S. Peiser of the National Bureau of Standards for assistance in preparing the manuscript, and to Dr. L. Walter (N.A.S.A. Goddard Spaceflight Center) for providing unpublished data and valuable discussion. Dr. K. H. Butler (Sylvania Lighting Products, Inc.) performed infrared analyses.

This research was supported in part by a Grant (SD-88) from the Advanced Research Project Agency (Ito) and in part by National Science Foundation Grant GA-1130 (Arem).

## REFERENCES

- AREM, J. E. (1967) Construction of tetrahedral models to aid visualization of multicomponent systems. *J. Geol. Educ.* **15**, 66-68.
- BARTH, T. F. W. (1963) Contribution to the mineralogy of Norway. No. 22, Vesuvianite from Kristiansand, other occurrences in Norway, the general formula of vesuvianite. *Norsk Geol. Tidsskr.* **43**, 457-472.
- BURNHAM, CHARLES W. (1962) Lattice constant refinement. *Carnegie Inst. Wash. Year Book* **61**, 132-135.
- BURNHAM, C. WAYNE (1959) Contact metamorphism of magnesian limestone at Crestmore, California. *Geol. Soc. Amer. Bull.* **70**, 879-920.
- CHRISTIE, O. H. J. (1961) On sub-solidus relations of silicates. 1. The lower breakdown temperature of the åkermanite gehlenite mixed crystal series at moderate water pressure. *Norsk Geol. Tidsskr.* **41**, 255-270.
- CHRISTOPHE-MICHEL-LÉVY, M. (1960) Reproduction artificielle de l'idocrase. *Bull. Soc. Franc. Mineral. Cristallogr.* **83**, 23-25.
- COES, L., JR. (1955) High pressure minerals. *J. Amer. Ceram. Soc.* **38**, 298.
- DE, A. (1961) *Petrology of Dikes Emplaced in the Ultramafic Rocks of Southeastern Quebec*. Ph.D. Thesis, Princeton University.
- DEER, W. A., R. A. HOWIE AND D. J. ZUSSMAN (1962) *Rock-forming minerals. Vol. 1*, John Wiley and Sons, Inc., New York, p. 114.
- DOWTY, E. AND R. MARK (1968) Application of Mössbauer and infrared spectroscopy to the crystal chemistry of natural titanium garnets. *Geol. Soc. Amer. Meet. Abstr.*, 80.
- GREENWOOD, H. J. (1962) Metamorphic reactions involving two volatile components. *Carnegie Inst. Wash. Year Book* **61**, 82-85.
- HAÛY, R. (1797) Sur les pierres appellées jusqu'ici hyacinthe et jargon de Ceylan. *J. Mines*, **5**, 260.
- HURLBUT, C. S., JR. (1955) Beryllian idocrase from Franklin, New Jersey. *Amer. Mineral.* **40**, 118-120.
- INOUE, T. AND A. MIYASHIRO (1951) Occurrences of vesuvianite in nepheline-syenite rocks of the Fukushinzan district, Korea; with general consideration of the relation between the composition and occurrence of vesuvianite. *J. Geol. Soc. Japan* **57**, 51-57.
- ITO, J. AND H. JOHNSON (1968) Synthesis and study of yttrialite. *Amer. Mineral.* **53**, 1940-1952.
- KURBATOV, S. M. (1922) Les vesuvianites des gisements russes. *Bull. Acad. Sci. Russie*, Ser. 6, **16**, 411-424.
- MACHATSCHKI, F. (1932) Zur Formel des Vesuvian. *Z. Kristallogr.* **81**, 148-152.
- MCCONNELL, D. (1939) Note on the chemical similarity of idocrase and certain garnets. *Amer. Mineral.* **24**, 62-63.
- MEEN, V. B. (1939) Vesuvianite from Great Slave Lake region, Canada. *Univ. Toronto Stud. Geol. Ser.* **42**, 69-73.
- NEUMANN, H. AND S. SVINNDAL (1965) The cyprine-thulite deposit at Ovstebo near Kleppan in Sauland, Telemark. *Norsk Geol. Tidsskr.* **34**, 139-156.
- PARRISH, W. (1960) Results of the I. U. Cr. precision lattice parameter project. *Acta Crystallogr.* **13**, 838-850.
- RAPP, G. AND J. V. SMITH (1958) Synthesis of idocrase (abstr.) *Bull. Geol. Soc. Amer.* **69**, 1741.

- SHABYNIN, L. I. (1968) The geochemical conditions for formation of idocrase in skarns. *Geokhimiya*, **10**, 1195-1210.
- SHANNON, R. D. AND C. T. PREWITT (1969) Effective ionic radii in oxides and fluorides. *Acta Crystallogr.* **B25**, 925-946.
- TURNER, F. J. AND J. VERHOOGEN (1960) *Igneous and Metamorphic Petrology*. McGraw-Hill Book Co., Inc. New York, 964 pp.
- WALDBAUM, D. R. (1966) *Colorimetric Investigation of Alkali Feldspars*. Ph.D. Thesis, Harvard University, 247 pp.
- WALTER, L. (1966) Synthesis and composition of idocrase in the system CaO-MgO-Al<sub>2</sub>O<sub>3</sub>-SiO<sub>2</sub>-H<sub>2</sub>O. *Geol. Soc. Amer. Ann. Meet. Program Abstr.*, **235**.  
(1968) (Private communication).
- WARREN, B. E. AND D. I. MODELL (1931) The structure of vesuvianite Ca<sub>10</sub>Al<sub>4</sub>(Mg, Fe)<sub>2</sub>Si<sub>13</sub>O<sub>18</sub>(OH)<sub>4</sub>. *Z. Kristallogr.* **78**, 422-432.

*Manuscript received, September 5, 1969; accepted for publication, January 17, 1970.*